Conversion $K_{WIOM/G}$ to saturation concentration (C*, µg/m³)

According to Donahue et al. (2006), $K_{org/G}'$ can be converted to C_i^* through :

$K_{org/G}' = 1/C_i^*$

Where $K_{org/G}'$ is partitioning coefficient between organic and gas phase in units of m³ (air) /µg (absorbing organics). If we assume the density of the absorbing organics is 1 g/cm³ (i.e., 10^{12} µg/m³), then the following should hold:

$K_{WIOM/G} = K_{org/G}' \cdot 10^{12}$ (µg/m³) = $1/C^* \cdot 10^{12}$ (µg/m³)

Conversion of $K_{W/G}$ to Henry's constant (K_H) in unit M/atm

Henry's constant (K_H in unit of M/atm) can be converted to $K_{W/G}$ according to the following relationship:

$K_{W/G} = K_H \cdot R \cdot T$

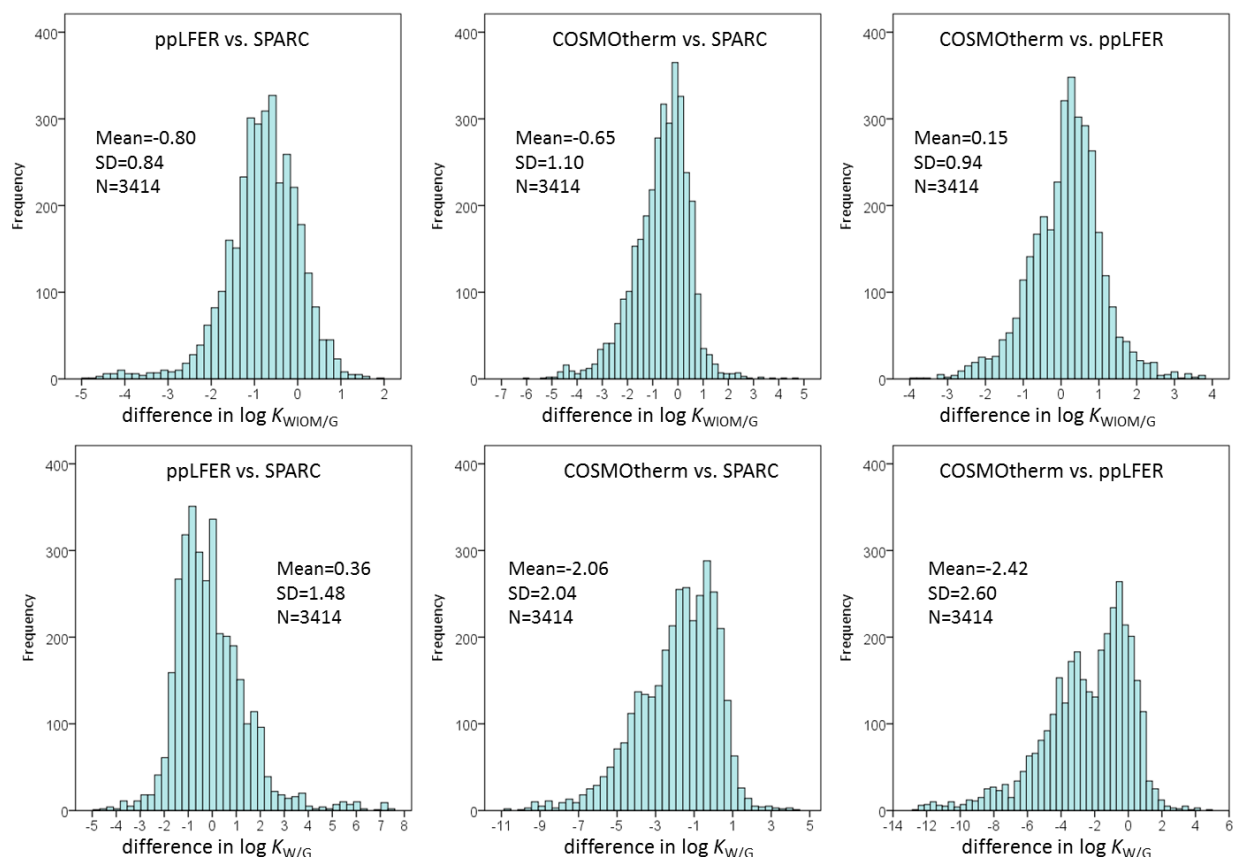Where R is the gas constant in unit of L atm K^{-1} mol^{-1} and T is temperature in K.
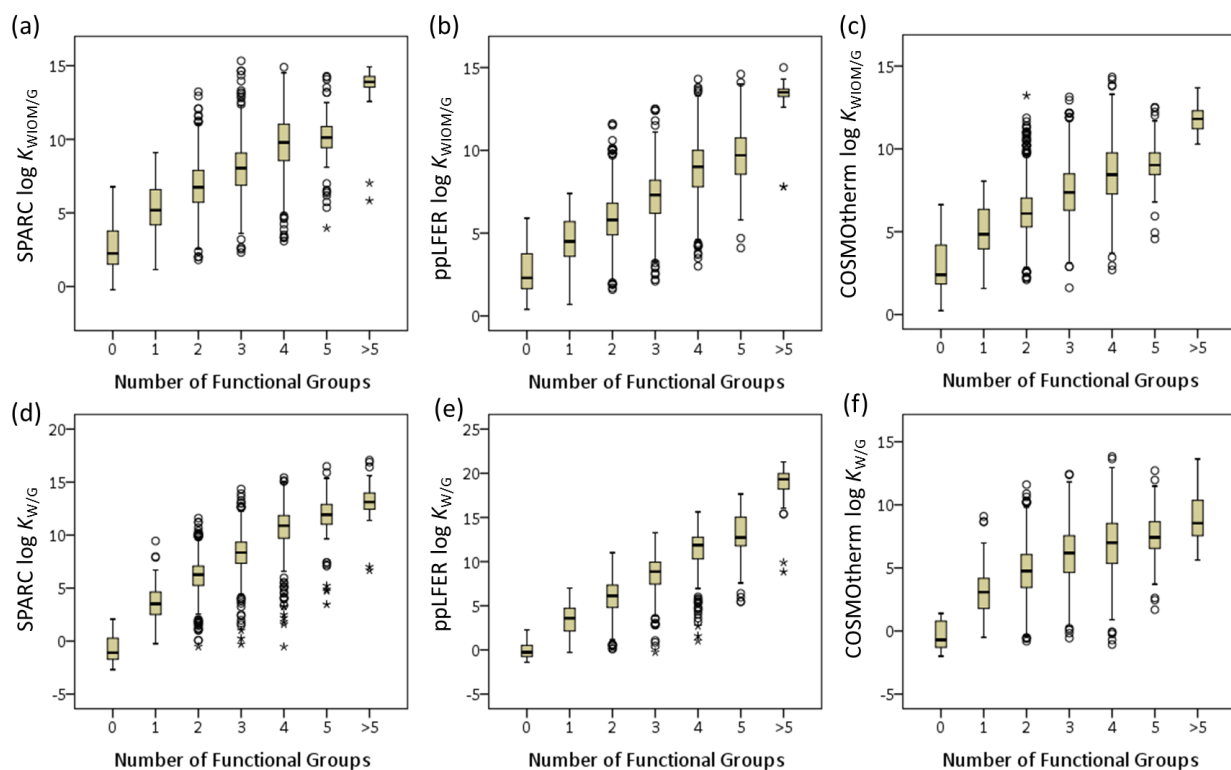
Figure S2   Boxplot of log $K_{WIOM/G}$ (upper panel) and log $K_{W/G}$ (lower panel) for compounds with different number of functional groups. The line inside each box (and the number on the side) shows the median of log $K_{WIOM/G}$ or log $K_{W/G}$ for different categories of compounds. The marker circle and star indicates possible outliers and extreme values, respectively.
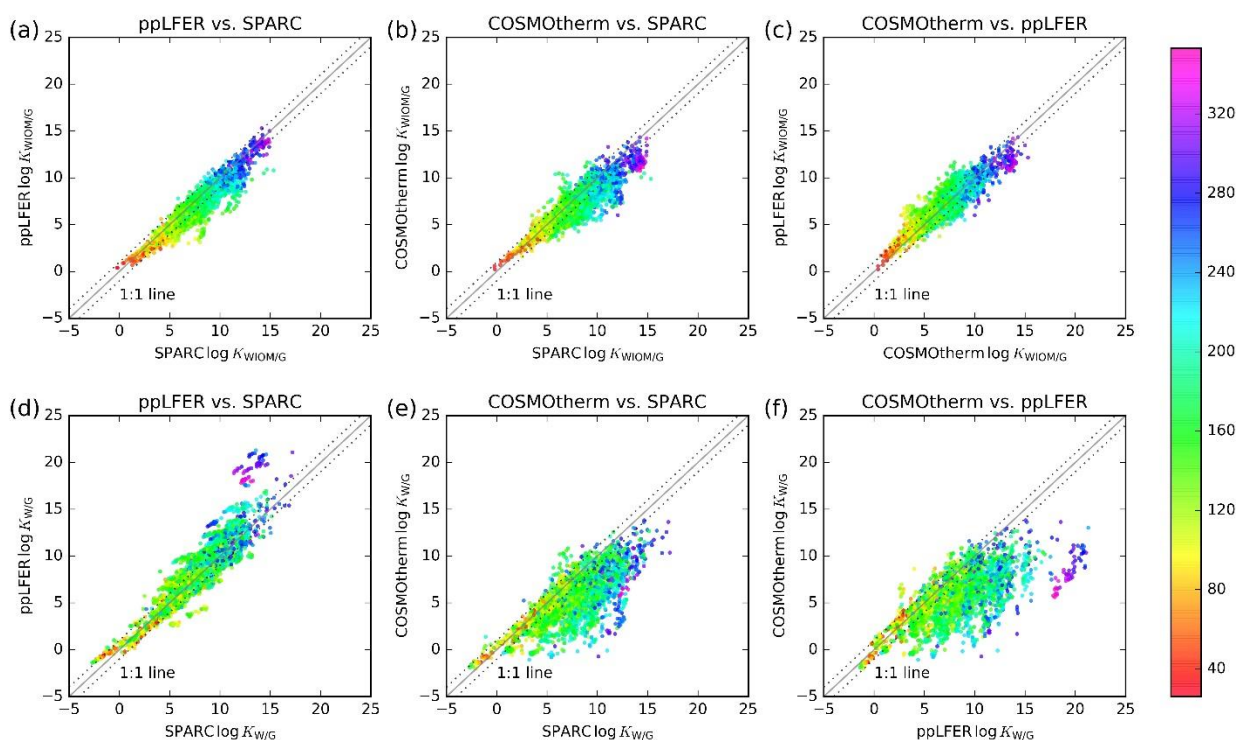
Figure S3   Comparison of the $K_{WIOM/G}$ (upper panel) and $K_{W/G}$ (lower panel) predicted using COSMOtherm, SPARC and ppLFERs. The solid line indicates a 1:1 agreement. The dotted lines indicate the deviation by ±1 log unit. The color scale indicates the molecular mass of the molecules (in units of g/mol).
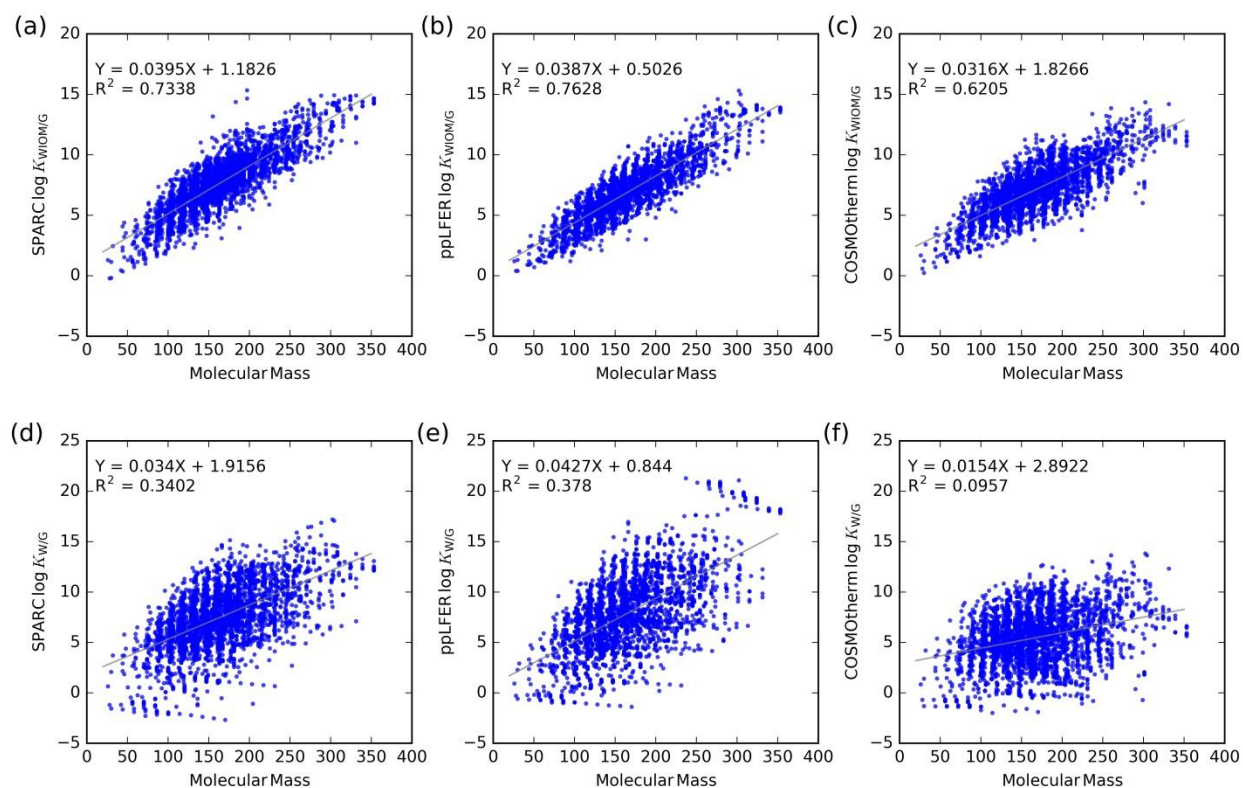
Figure S4   Correlation of predicted $K_{WIOM/G}$ (upper panel) and $K_{W/G}$ (lower panel) with the molecular mass (in units of g/mol). The lines show the regressions of partitioning coefficients with molecular mass. Also shown are the regression equations.
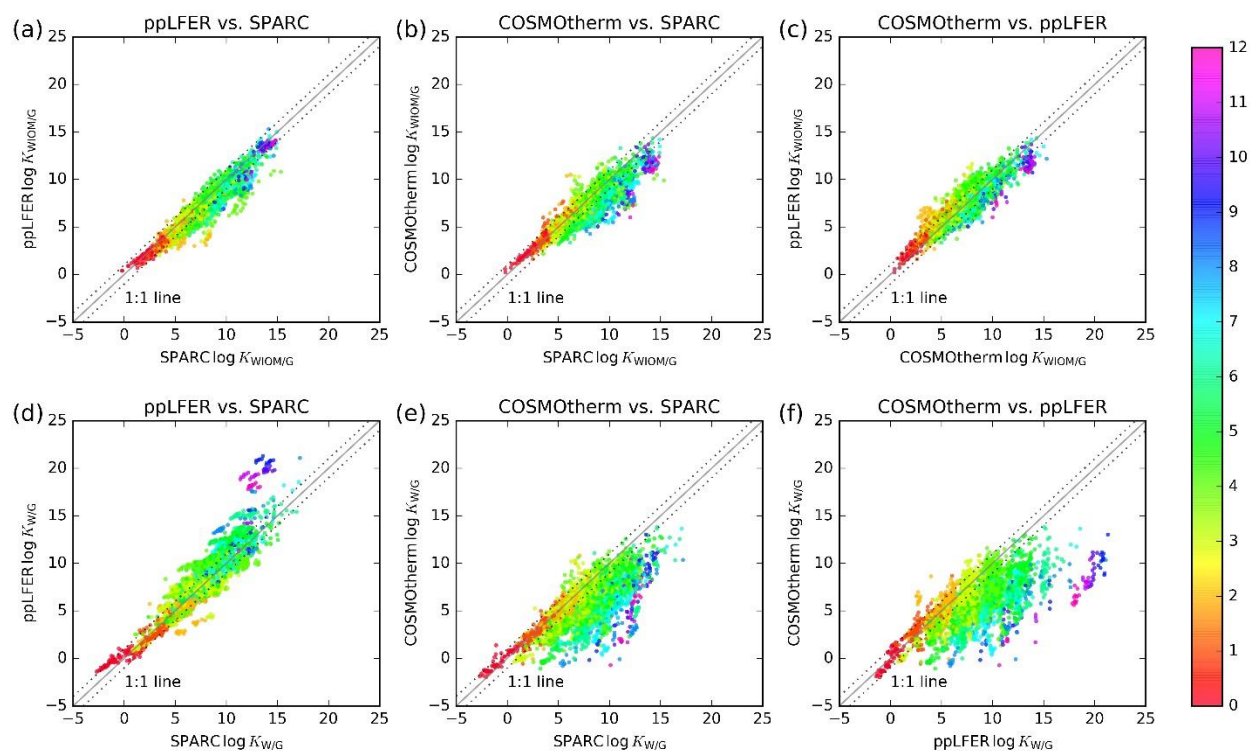
Figure S5 Comparison of the $K_{WIOM/G}$ (upper panel) and $K_{W/G}$ (lower panel) predicted using COSMOtherm, SPARC and ppLFERs. The color scale indicates the number of oxygen in the molecules. The solid line indicates a 1:1 agreement. The dotted lines indicate the deviation by ±1 log unit.
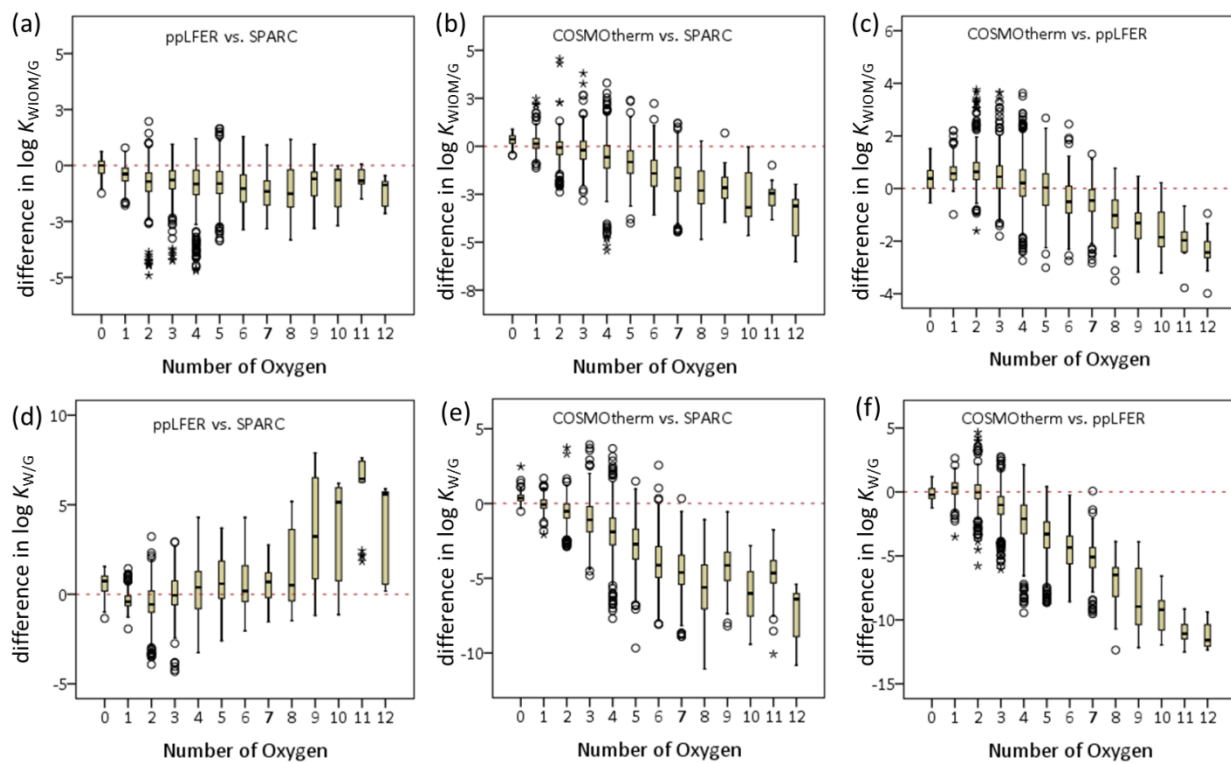
Figure S6   Boxplot of difference in SPARC, ppLFER and COSMOtherm predictions for compounds with different number of oxygens. The line inside each box shows the median difference for log $K_{WIOM/G}$ or log $K_{W/G}$ for different categories of compounds. The marker circle and star indicates possible outliers and extreme values, respectively.
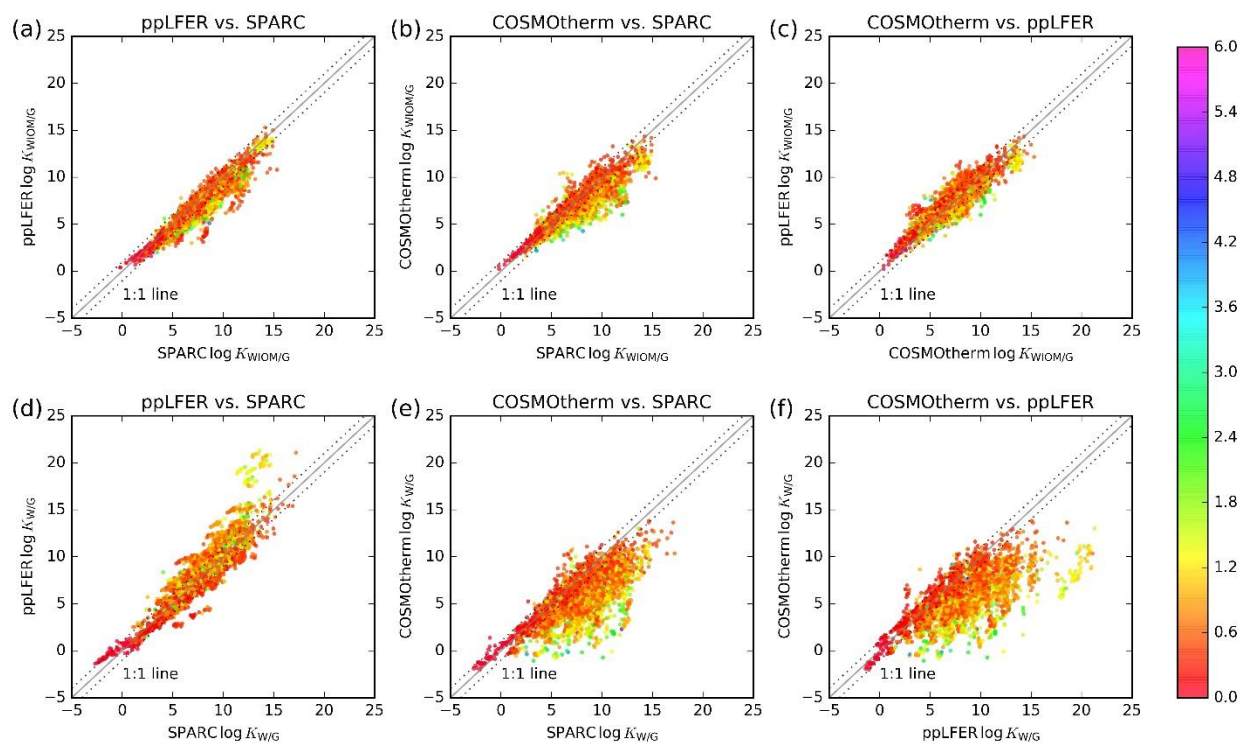
Figure S7   Comparison of the $K_{WIOM/G}$ (upper panel) and $K_{W/G}$ (lower panel) predicted using COSMOtherm, SPARC and ppLFERs. The color scale indicates the O:C ratio of the molecules.
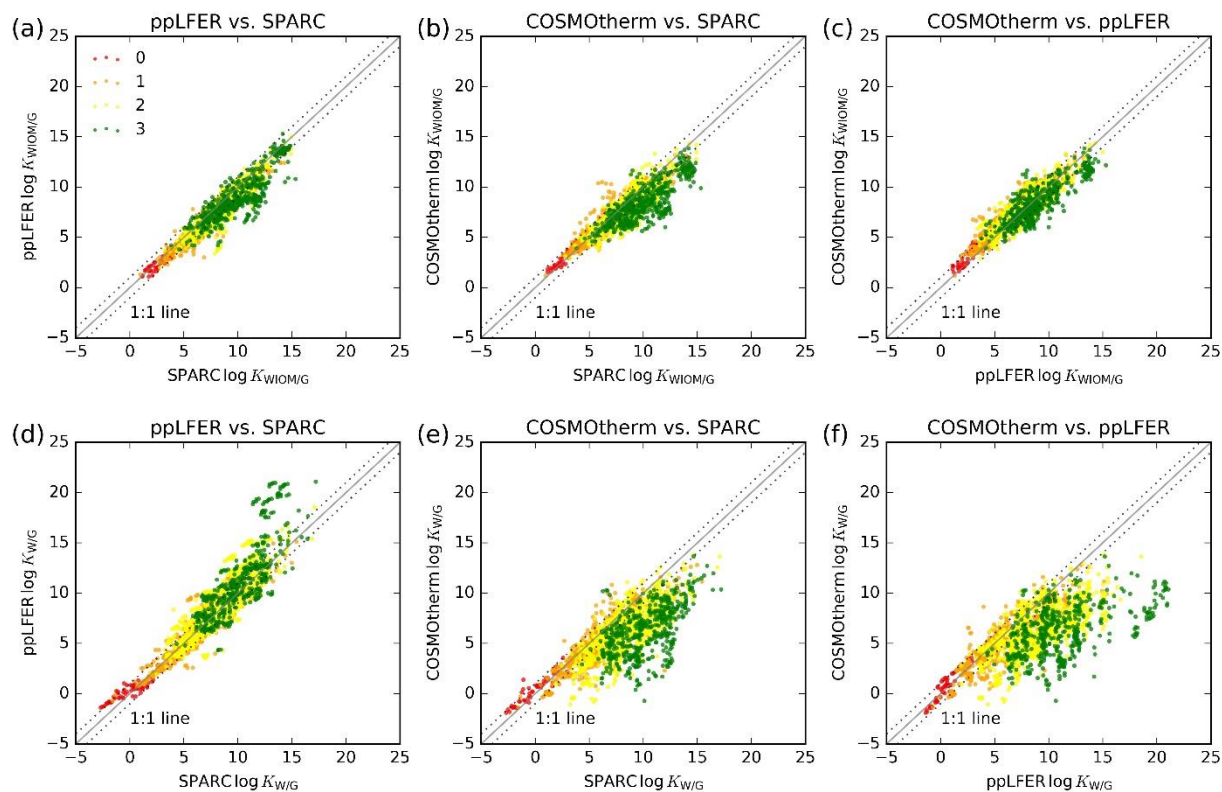
Figure S8   Comparison of the $K_{WIOM/G}$ (upper panel) and $K_{W/G}$ (lower panel) predicted using COSMOtherm, SPARC and ppLFERs. The color scale indicates the generation of oxidation of the molecules. The oxidation generation information is available for 2148 compounds among all. Compound with an oxidation generation of 0 (i.e., OXGEN=0, the red dots) are precursor compounds.
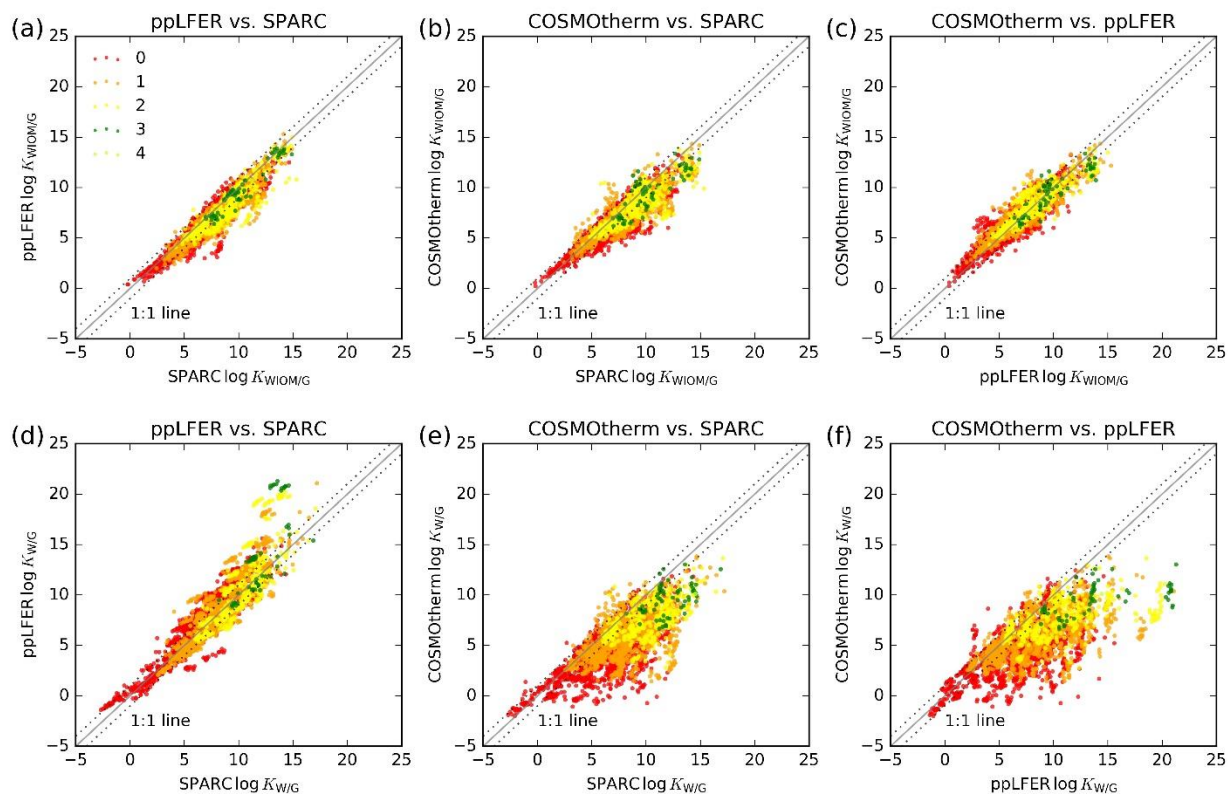
Figure S9   Comparison of the $K_{\text{WIOM/G}}$ (upper panel) and $K_{\text{W/G}}$ (lower panel) predicted using COSMOtherm, SPARC and ppLFERs. The color scale indicates the number of OH in the molecules.
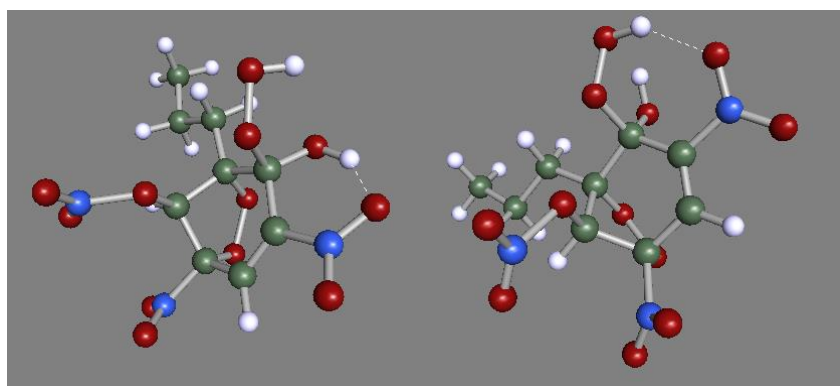

Figure S10   Two conformers for an organic compound (MCM ID: NDNPBZLOOH). COSMOconf calculated six conformers for this compound and two are shown here as an example of intra-molecular interactions.
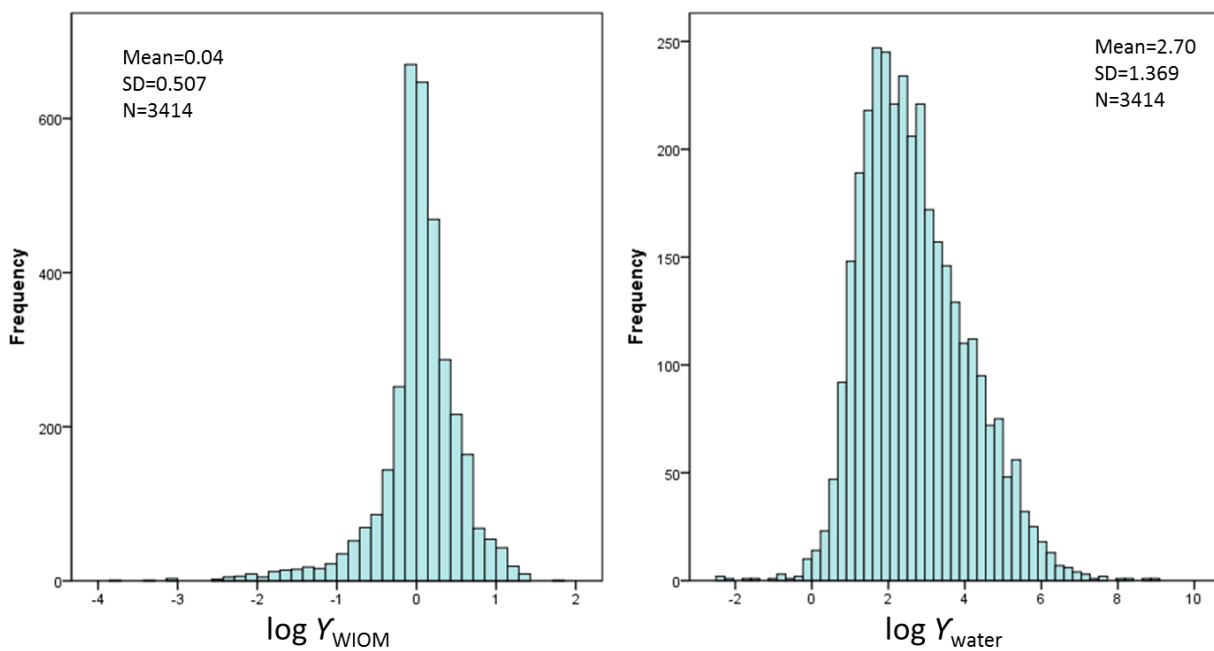
Figure S11   Histogram of log Y_{WIOM} and log Y_{water} for 3414 organic compounds.

Description of the Partitioning Space

Figure S12 are chemical partitioning space maps, showing the combinations of partitioning properties that lead to dominant equilibrium partitioning to the gas (pink), aqueous (blue), and water insoluble organic matter phases (green), respectively. Four scenarios are assessed, with panel (a) representing an aerosol scenario (LWC 10 $\mu g/m^3$, 10 $\mu g/m^3$ OM), (b) representing a cloud scenario (LWC 0.3 g/m^3, 10 $\mu g/m^3$ OM), (c) representing an aerosol scenario without a separated aqueous phase (LWC 0 $\mu g/m^3$, 10 $\mu g/m^3$ OM) and (d) representing a cloud scenario without a separated WIOM phase (LWC 0.3 g/m^3, 0 $\mu g/m^3$ OM). The dotted lines in the space indicate boundaries for different fractions of compounds in each phase. For instance, a compound with a log $K_{W/G}$ of 11 and a log $K_{WIOM/G}$ less than 10 (i.e. on the boundary line between the light pink and light blue region) would have 50 % each in either the gas or aqueous phase. The white color triangle in (a) and (b) shows the transition region where less than 50 % are present in each of the three phases.
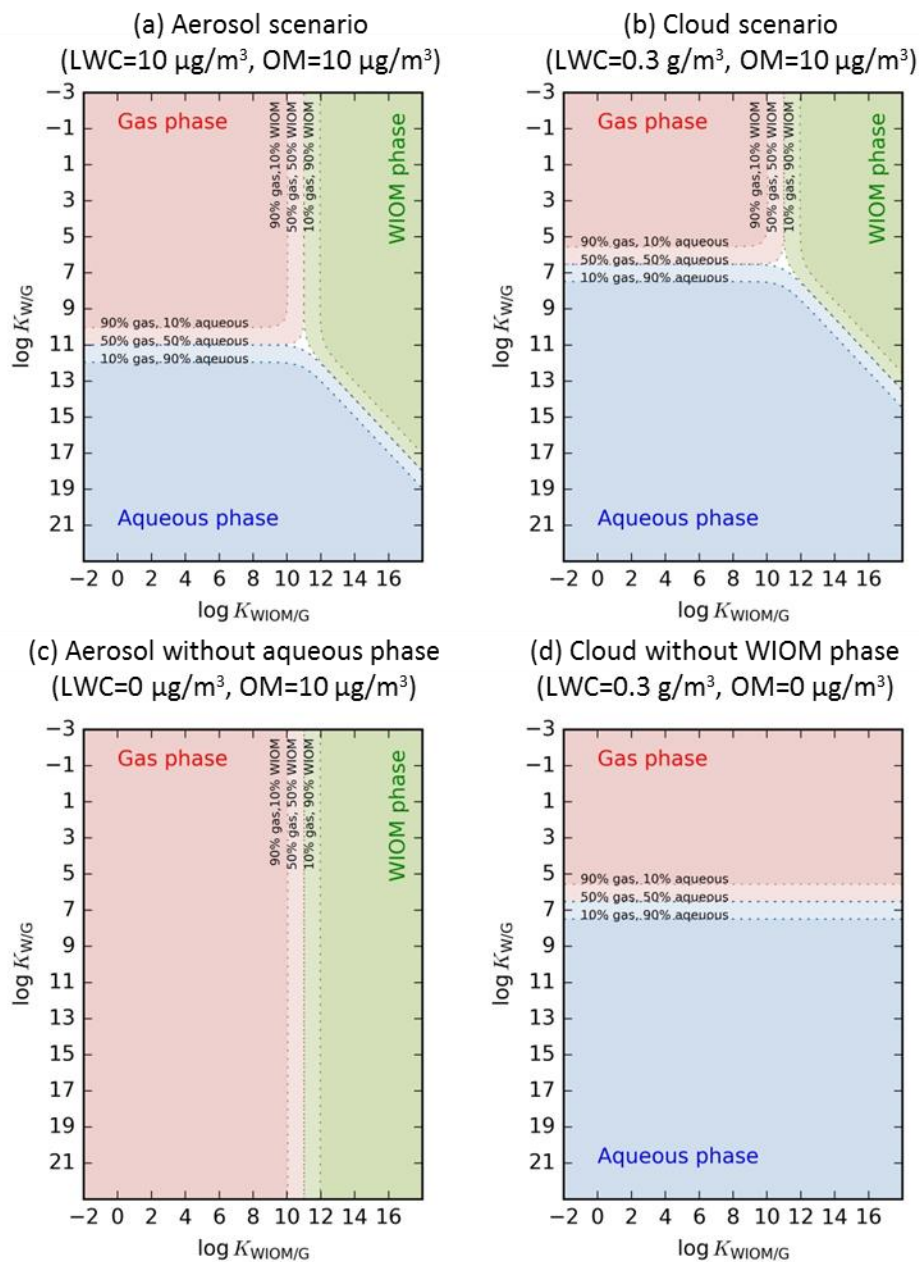
Figure S12 Partitioning space map for aerosol (a), cloud (b), aerosol without aqueous phase (c) and cloud without WIOM phase (d)
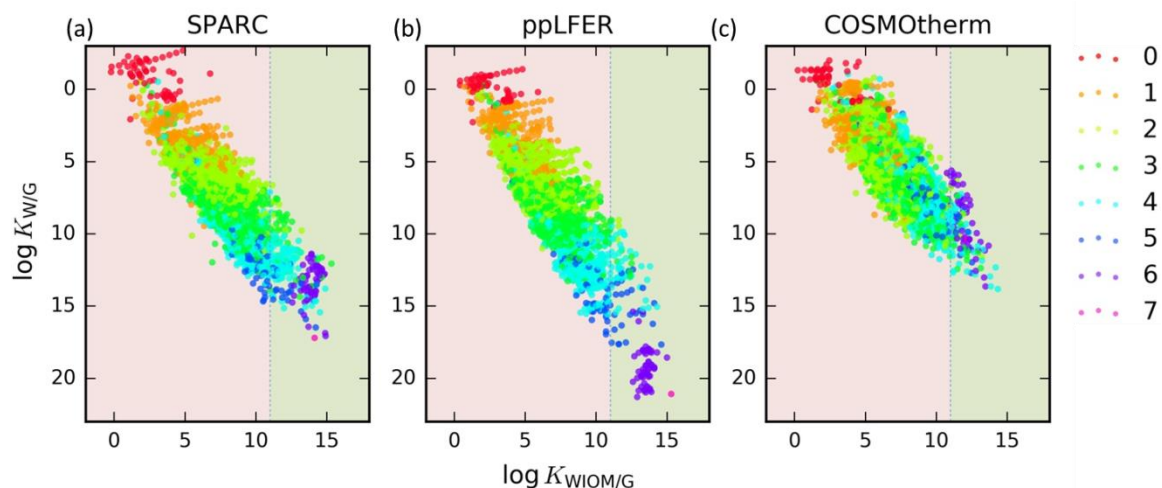
Figure S13   Partitioning space plot, showing in pink and green the combinations of partitioning properties that lead to dominant equilibrium partitioning to the gas and WIOM phases, respectively. The blue dotted lines are boundaries for an aerosol scenario without an aqueous phase (LWC 0 µg/m^3, 10 µg/m^3 OM). The differently colored dots indicate the number of functional groups in the molecules
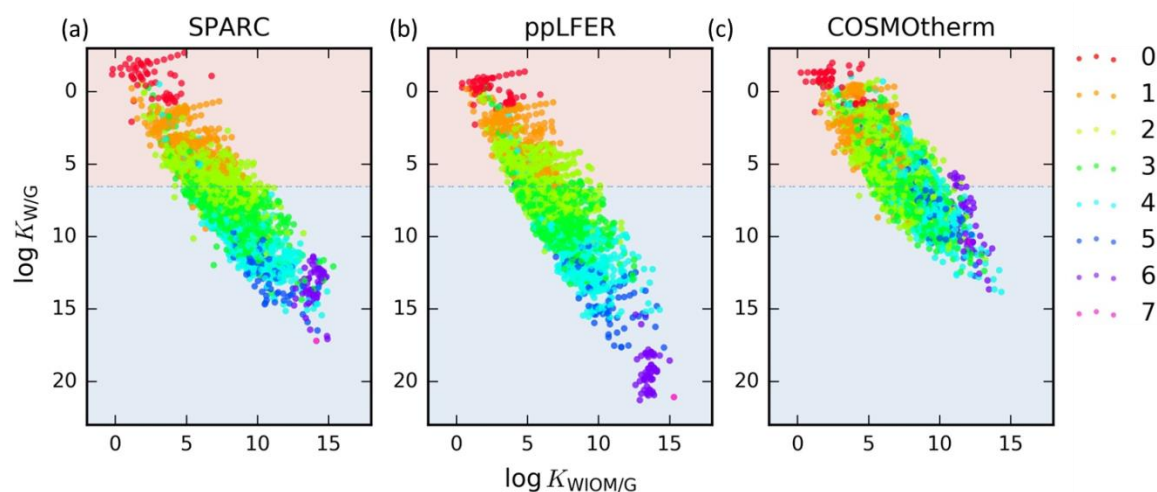

Figure S14   Partitioning space plot, showing in pink and blue the combinations of partitioning properties that lead to dominant equilibrium partitioning to the gas and aqueous phases, respectively. The horizontal blue dashed lines a cloud scenario where LWC is 0.3 g/m^3 and OM 0 µg/m^3. The differently colored dots indicate the number of functional groups in the molecules
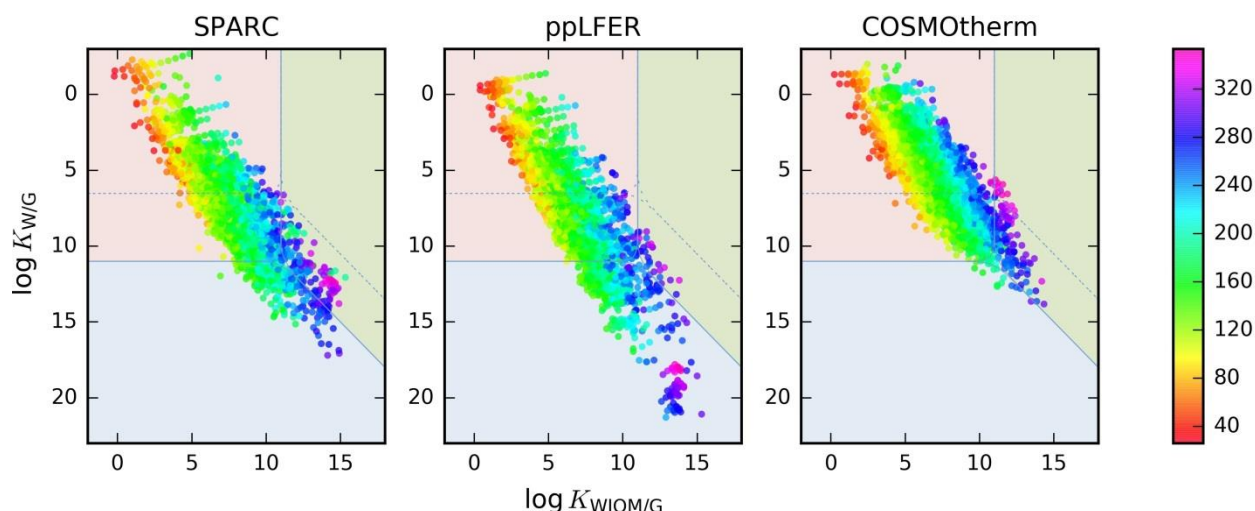
Figure S15   Partitioning space plot, showing in pink, blue and green the combinations of partitioning properties that lead to dominant equilibrium partitioning to the gas, aqueous and WIOM phases, respectively. The solid and dotted lines are boundaries for an aerosol scenario (LWC 10 μg/m^3, 10 μg/m^3 OM) and a cloud scenario (LWC 0.3 g/m^3, 10 μg/m^3 OM), respectively. The color scale indicates the molecular mass of the molecules.

Table S1   Number (percentage) of compounds change from predominantly partitioning to gas phase to condensed phase when a different prediction method is used under different atmospheric conditions

(a) aerosol (LWC=10 μg/m^3, OM=10 μg/m^3)			(c) aerosl without water (LWC=0 μg/m^3, OM=10 μg/m^3)		
from ppLFER to SPARC	from SPARC to ppLFER	total change	from ppLFER to SPARC	from SPARC to ppLFER	total change
107 (3.1%)	195 (5.7%)	302 (8.8%)	146 (4.3 %)	11 (0.3%)	157 (4.6%)
from ppLFER to COSMOtherm	from COSMOtherm to ppLFER	total change	from ppLFER to COSMOtherm	from COSMOtherm to ppLFER	total change
17 (0.5%)	481 (14.1 %)	498 (14.6%)	26 (0.8%)	41 (1.2%)	67 (2.0%)
from SPARC to COSMOtherm	from COSMOtherm to ppLFER	total change	from SPARC to COSMOtherm	from COSMOtherm to SPARC	total change
12 (0.4%)	388 (11.4%)	400 (11.7%)	14 (0.4%)	164 (4.8%)	178 (5.2%)
(b) cloud (LWC=0.3 g/m^3, OM=10 μg/m^3)			(d) cloud non-phase separated (LWC=0.3 g/m^3, OM=0 μg/m^3)		
from ppLFER to SPARC	from SPARC to ppLFER	total change	from ppLFER to SPARC	from SPARC to ppLFER	total change
166 (4.9%)	207 (6.1%)	373 (10.9%)	167 (4.9%)	206 (6.0%)	373 (10.9%)
from ppLFER to COSMOtherm	from COSMOtherm to ppLFER	total change	from ppLFER to COSMOtherm	from COSMOtherm to ppLFER	total change
46 (1.3%)	1103 (32.3 %)	1149 (33.7%)	47 (1.4%)	1111 (32.5%)	1158 (33.9%)
from SPARC to COSMOtherm	from COSMOtherm to SPARC	total change	from SPARC to COSMOtherm	from COSMOtherm to SPARC	total change
40 (1.2%)	1056 (30.9 %)	1096 (32.1%)	40 (1.2%)	1065 (31.2%)	1105 (32.4%)

*The column "total change" indicates total number (percentage) of compounds that have different predicted dominant phases using different methods.

References

Donahue, N. M., Robinson, A. L., Stanier, C. O., and Pandis, S. N.: Coupled partitioning, dilution, and chemical aging of semivolatile organics, Environmental Science & Technology, 40, 2635-2643, 10.1021/es052297c, 2006.